HNPS Advances in Nuclear Physics

Vol 32 (2026)

HNPS2025

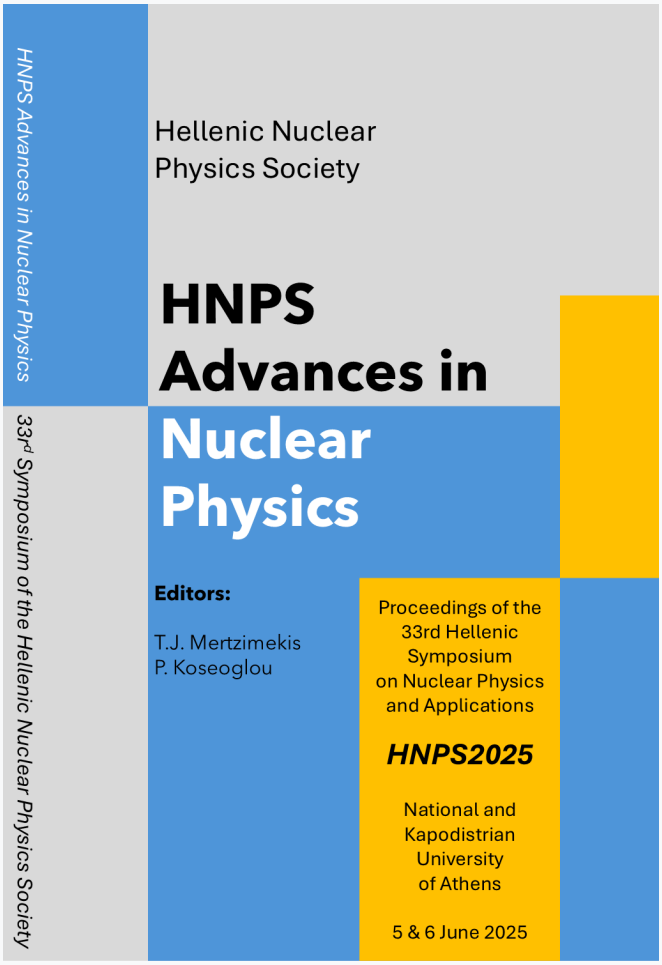

Multinucleon Transfer in Peripheral Collisions of 64Ni on 64Ni at 25 MeV/nucleon

Eirini Kontogianni, Georgios A. Souliotis, Chrysi Giannitsa, Konstantinos Gkatzogias, Stergios Koulouris, Eleftheria Travlou, Martin Veselsky, Sherry J. Yennelo, Aldo Bonasera

doi: 10.12681/hnpsanp.8865

To cite this article:

Kontogianni, E., Souliotis, G. A., Giannitsa, C., Gkatzogias, K., Koulouris, S., Travlou, E., Veselsky, M., Yennelo, S. J., & Bonasera, A. (2026). Multinucleon Transfer in Peripheral Collisions of 64Ni on 64Ni at 25 MeV/nucleon. *HNPS Advances in Nuclear Physics*, *32*, 198–204. https://doi.org/10.12681/hnpsanp.8865

HNPS Advances in Nuclear Physics Vol. **32**, 198–204 (2025)
doi: 10.12681/hnpsanp.8865

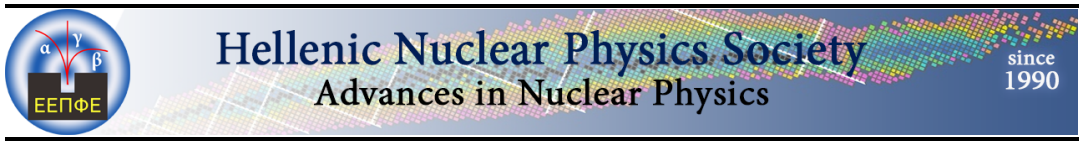

ARTICLE

Multinucleon Transfer in Peripheral Collisions of ^{64}Ni on ^{64}Ni at 25 MeV/nucleon

E. Kontogianni,[*,1] G.A. Souliotis,[1] Ch. Giannitsa,[1] K. Gkatzogias,[1] S. Koulouris,[1] E. Travlou,[1] M. Veselsky,[2] S.J. Yennello,[3] and A. Bonasera[3]

[1]Laboratory of Physical Chemistry, Department of Chemistry, National and Kapodistrian University of Athens, Athens, Greece
[2]Institute of Experimental and Applied Physics, Czech Technical University, Prague, Czech Republic
[3]Cyclotron Institute, Texas A&M University, College Station, Texas, USA
*Corresponding author: eirinikont@chem.uoa.gr

(Received: 09 Nov 2025; Accepted: 31 Jan 2026; Published: 02 Feb 2026)

Abstract
We study the yields, the momentum distributions and the angular distributions of projectile-like fragments from peripheral collisions of ^{64}Ni (25 MeV/nucleon) on ^{64}Ni. The experimental data were obtained in previous works with the BigSol separator system at the Cyclotron Institute of Texas A&M University. Projectile fragments were collected and analyzed at forward angles (1.5°-3.0°). The production cross sections, the momentum distributions and the angular distributions of the fragments were systematically studied and compared with the Deep-Inelastic Transfer (DIT) model and the Constrained Molecular Dynamics (CoMD) model followed by the deexcitation model GEMINI. Both models appear to describe the data rather adequately, but possible improvements are necessary. Special attention is given in the possibility to produce neutron-rich rare isotopes of elements at the beginning of the astrophysical r-process. Moreover, efforts similar to this work are ongoing to shed light to the reaction mechanisms of peripheral collisions at this energy (25 MeV/nucleon).

Keywords: Multinucleon Transfer; Peripheral Collisions; Yields; Momentum Distributions; Angular Distributions

1. Introduction

The exploration of neutron rich nuclides, far from the beta stability valley of the nuclear chart, is expected to yield valuable insights into nuclear structure as the N/Z ratio increases, while also shedding light on nucleosynthetic processes, such as the rapid neutron capture process (r-process) [1]. Therefore, it is of particular importance to investigate the reaction mechanisms responsible for the production of such neutron-rich isotopes [2]. By analyzing observables, such as fragment yields, momentum distributions and angular distributions, we can gain a deeper understanding of the dynamics governing peripheral heavy-ion collisions in the Fermi energy range (15-25 MeV/nucleon).

 ISBN 2654-007X (print), 2654-0088 (online).

Such studies, also, provide guidance for optimizing the production of neutron-rich nuclides [3–5]. In the present work, we focus on the projectile-like fragment distributions emerging from the reaction ^{64}Ni (25 MeV/nucleon) on ^{64}Ni. The dynamical stage of the reaction was described using two approaches, the Deep Inelastic Transfer (DIT) model [6] and the Constrained Molecular Dynamics (CoMD) model [7]. In both cases, the subsequent de-excitation stage of the reaction was performed by the statistical decay code, GEMINI [8]. Section 2 outlines the overview of the experimental setup and the data collection. Section 3 briefly reviews the theoretical models employed and section 4 presents the experimental results along with a comparison to our theoretical calculations. Finally, section 5 summarizes our conclusions.

2. Experimental Setup and Data Analysis

The experimental data analyzed in this study were collected at the Cyclotron Institute of Texas A&M University with part of the dataset reported in detail in previous works [9–11]. A brief overview of the experimental set-up is provided. The ^{64}Ni (25 MeV/nucleon) beam was produced by an ECR (Electron Cyclotron Resonance) ion source and accelerated by the K500 Cyclotron followed by its interaction with a ^{64}Ni (4 mg/cm^2) target. The collection of the projectile-like fragments was performed with the Superconducting Solenoid Line (BigSol). The main component of the line is the large bore 7 Tesla superconducting solenoid of the University of Michigan. A schematic diagram of the line is illustrated in Fig. 1. A primary production target is positioned 1 m upstream of the solenoid and is bombarded with the ^{64}Ni beam. The unreached beam is collected on a cylindrical Faraday cup placed at a distance of 30 cm after the target. The geometry and the kinematics of the device are selected in such way that fragments emitted within an angular range of 1.5°-3.0°, passed through a stripper foil, traversed the solenoid and were focused 4 m after it (intermediate image). At this location, a magnetic rigidity $B\rho = \frac{p}{q}$ acceptance of ~4% was defined with another circular aperture. Detection systems were arranged at both the intermediate and the final image positions. Specifically, the first of the two xy position-sensitive Parallel Plate Avalanche Counters (PPAC) are located in the intermediate image, while the fragments are subsequently transported through a 7.5 m line and focused with the aid of the quadrupole triplet at the end of the line (final image), where the other PPAC is located. The Time of flight (TOF) was measured between the two PPAC detectors. Finally, the fragments are focused at the end of the setup in a four-element (ΔE1,ΔE2,E1,E2) Si detector telescope. This provided measurements of energy loss and residual energy, which, combined with the TOF information (with resolution ~0.5%), enabled the determination of both charge and mass number. It should be emphasized that the mass determination in this work relied exclusively on the measurement of the total energy and TOF. This is due to the fact that BigSol does not operate as a high-resolution $\frac{p}{q}$ dispersive spectrometer; its components function purely as focusing elements rather than dispersion elements. Nevertheless, a radial $\frac{p}{q}$ dispersion exists at the intermediate image of the solenoid (and likewise at the final image, owing to the quadrupole triplet) resulting in the dependence of the focal position on $\frac{p}{q}$. This dispersion is also a function of the initial angle. The measurement of the radial distance of the fragments at the intermediate image (emerging, in the initial angular range of 1.5°-3.0°), combined with the value of the central magnetic field of the solenoid, provided a $\frac{p}{q}$ determination with a resolution of ~2%. Although this precision is insufficient for accurate mass determination, it was adequate to determine the ionic charge state q. A series of runs was carried out at overlapping magnetic rigidity settings of the spectrometer in the range 1.1-1.6 Tm for the ^{64}Ni (25 MeV/nucleon) on ^{64}Ni reaction. The collected data were normalized and appropriately combined. After summation over all ionic charge states and subsequent normalization to beam current and target thickness, the fragment yield distributions as a function of Z, A and velocity were extracted.

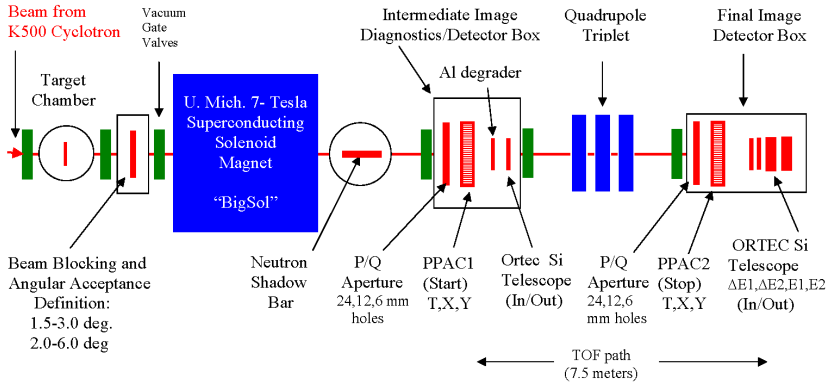

Figure 1. Superconducting Solenoid Separator at Texas A&M University (2003-2008) [9]

3. Theoretical Framework

The DIT model [6] is a phenomenological model designed to describe peripheral collisions. The target and the projectile are considered as spheres moving along Coulomb trajectories, until they are within the range of the nuclear interaction, where the system can be described as two Fermi gases in contact. The nuclei interact through their overlapping potentials. During that interaction, a "window" opens in the inter- nuclear potential that allows the stochastic exchange of nucleons.

The CoMD code [7] is a microscopic model. Based on Quantum Molecular Dynamics methods, it assumes that nucleons are described as Gaussian wavepackets interacting via an effective nucleon-nucleon interaction. The fermionic nature of the system is imposed by a phase-space constraint that enforces the Pauli principle at each time step of the system's evolution. The description of the de-excitation of the hot projectile-like fragments produced in the dynamic state of the reaction was performed by the code GEMINI [8], a statistical decay code developed to study sequential decays.

In both models, standard parameters have been used as they have been optimized by previous efforts [5].

4. Results and Discussion

The experimental results as well as their comparison with the theoretical calculations are presented in this part of the contribution. In Fig. 2, we show the mass distributions of projectile-like fragments produced in the reaction of ^{64}Ni with ^{64}Ni at 25 MeV per nucleon. The analyzed reaction channels correspond to fragments with atomic numbers between 23 and 30. The experimental data are represented by black points, while the DIT and CoMD model calculations are shown with blue and red lines, respectively. The dashed vertical green lines mark the onset of neutron pick-up. The experimental yields were extracted from the measured cross sections within the solid-angle acceptance of the detection setup ($d\Omega$ = 6.5 msr), which corresponds to an angular range of 1.5°-3.0°, and within the magnetic rigidity range covered by the experiment. To suppress the intense elastically scattered beam, specific magnetic rigidity regions had to be excluded; as a result, the collection of the most neutron-rich fragments near the projectile (Z = 27, 28) was incomplete.

The figure displays three versions of the DIT (blue) and CoMD (red) calculations. The dotted curves represent the primary fragments—highly excited precursors that, after de-excitation, lead to the so-

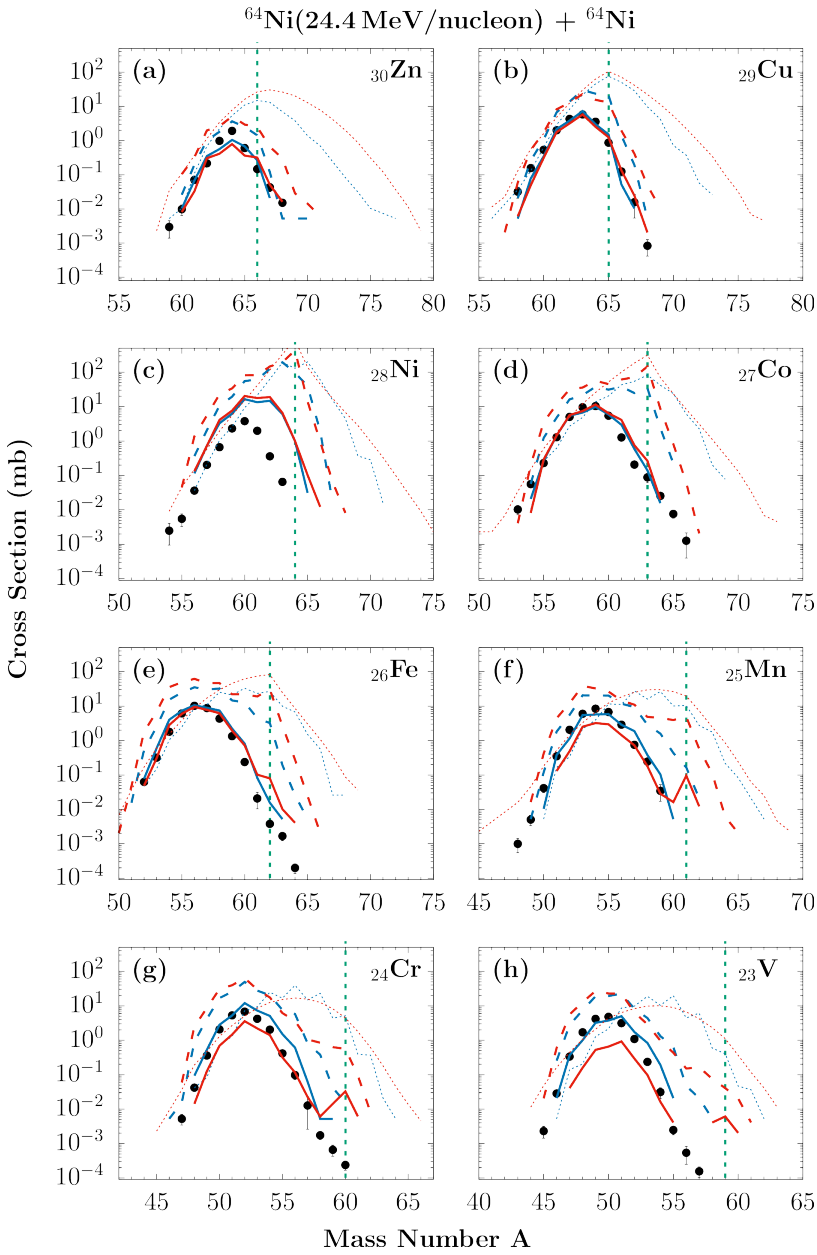

Figure 2. Mass distributions (cross sections) of projectile fragments from peripheral collisions of 25 MeV/nucleon ^{64}Ni on ^{64}Ni. The experimental data are shown by solid black points. The DIT calculations are represented by the blue lines and the CoMD calculations by the red lines. The dotted lines refer to the primary fragments, the dashed lines refer to the total cold products and the solid lines refer to the filtered cold products. The vertical green line shows the beginning of the neutron pick-up that develops to the right.

called "cold" nuclei, i.e., fragments de-excited below the neutron separation energy. These cold fragments are shown by the dashed curves and correspond to the full population potentially observable in an experiment. Because the BigSol spectrometer has limited angular and magnetic rigidity acceptance, the calculations were filtered according to these experimental constraints, with the resulting

distributions shown by the solid lines. Overall, several observations can be made. The primary fragments exhibit broad distributions extending toward very neutron-rich isotopes. The DIT and CoMD results are comparable, as illustrated by their direct comparison in the neutron-rich region of the panels of the figure. Importantly, the filtered "cold" fragment calculations reproduce the experimental data very well for nearly all isotopic chains, except for Ni, where discrepancies arise from additional magnetic rigidity cuts applied during the data analysis that were not incorporated into the software filtering procedure.

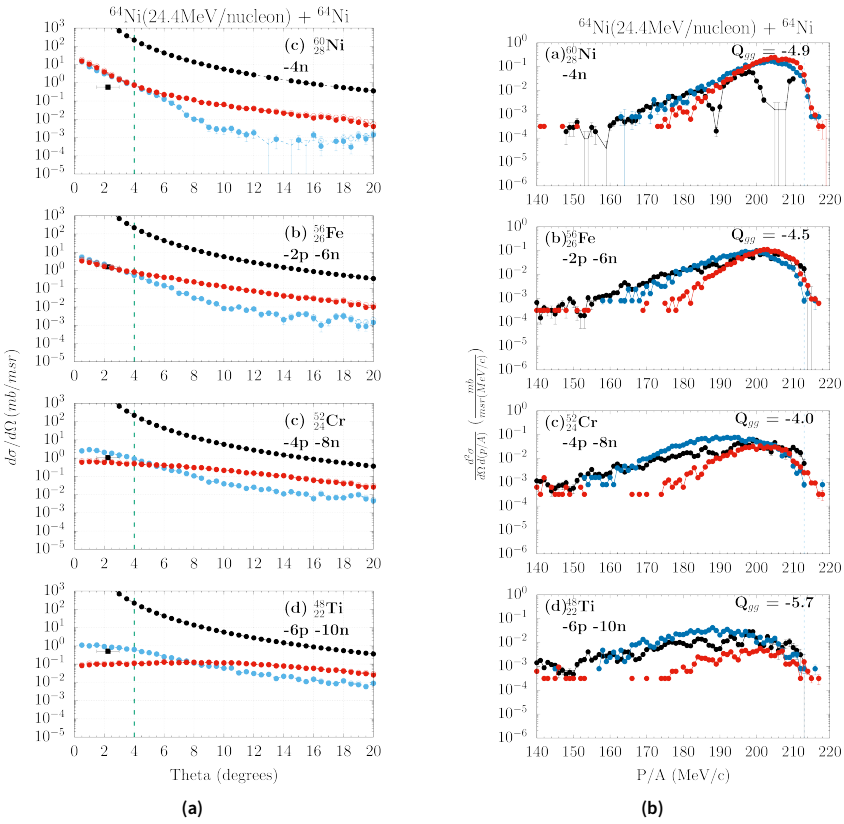

Figure 3. (a): Angular distributions of projectile-like fragments for peak isotope channels. The experimental data are shown by solid black squares and the Rutherford scattering is represented by black circles. The DIT calculation is represented by the blue points and the CoMD calculation by the red points. (b): Momentum per nucleon distributions of projectile fragments for peak isotope channels. The experimental data are shown by solid black points. The DIT calculation is represented by the blue points and the CoMD calculation by the red points. The vertical dashed (green) lines indicate the p/A of the projectile exiting the targets.

Both DIT and CoMD calculations reproduce the main features of the experimental mass distributions. The primary fragment distributions extend toward more neutron-rich isotopes and show higher cross sections than the corresponding cold fragments, reflecting nucleon and light-particle emission during de-excitation. After filtering for the experimental acceptance, the calculated final distributions exhibit very good agreement with the measured yields across most isotopic chains. The satisfactory reproduction of the data indicates that both models provide an adequate description of multinucleon transfer mechanisms in this energy regime. Notably, the data show the production of neutron-rich isotopes corresponding to up to three-neutron pick-up (particularly for Co and Cu), a feature that is well captured by both theoretical approaches. The DIT and CoMD results are overall consistent with each other and together they provide a coherent picture of the reaction dynamics

and fragment formation process.

In Fig. 3 we present the momentum per nucleon ($\frac{p}{A}$) distributions and angular distributions of projectile fragments for peak isotope channels from the reaction ^{64}Ni with ^{64}Ni target at 25 MeV/nucleon. Peak isotopes refer to the isotopes at the maximum of the yield distributions. Black points represent the experimental data. The DIT calculation is represented by blue points and the CoMD calculation by red points.

Regarding the momentum distributions, we note that the horizontal axis shows momentum per nucleon, which essentially represents velocity. The momentum per nucleon $\left(\frac{p}{A}\right)$ is a measure of the energy dissipation that takes place in the interaction of the target-projectile binary system and holds valuable information on the reaction mechanisms that lead to the production of the fragments of interest. The vertical axis gives the measured differential cross section $\frac{d^2\sigma}{d\left(\frac{p}{A}\right)d\Omega}$ in units of $\left[\frac{mb}{(MeV/c)\ msr}\right]$. Each panel represents a different reaction channel, as indicated. The experimental data in the -4n channel (Fig. 3) appear to have large gaps (empty regions) that are due to the exclusions of the elastically scattered projectiles in both the experimental measurement and the data analysis. The general feature of the $\frac{p}{A}$ distributions is the presence of two main regions, the quasi-elastic region that corresponds to direct processes and a broader region, located in lower values of $\left(\frac{p}{A}\right)$, that corresponds to more dissipative mechanisms. The total excitation energy of the quasi-projectile and quasi-target system was obtained by binary kinematics calculations assuming no nucleon evaporation.

In the angular distribution figures, the x-axis represents the angle of the projectile-like fragments and in the y-axis the differential cross section with respect to solid angle, ($d\Omega$) in units of $\left[\frac{mb}{msr}\right]$. The BigSol experimental apparatus measures in only one angle interval, 1.5°-3.0° so we have only one experimental point at each channel, represented by the black square. In each channel we also present the Rutherford scattering shown by black circles. The blue open circles represent the DIT calculations, the red open circles the standard CoMD calculations, while the blue full circles represent the DIT calculations, filtered for magnetic rigidity, as well as the red full circles represent the filtered CoMD calculations. In most cases, the DIT calculations seem to be slightly more efficient in describing the experimental data.

The DIT and CoMD calculations shown in Fig. 3 correspond to the "cold" filtered products (similar to the solid lines in Fig. 2). The calculations of Fig. 3b appear to describe the features of the experimental data. We plan to improve the model calculations in the near future and further understand the data versus calculations comparisons.

5. Conclusions

In this contribution we present our study of distributions of projectile-like fragments from the reaction of ^{64}Ni (25 MeV/nucleon) on ^{64}Ni target. Experimental data on production cross sections, momentum distributions and angular distributions were examined. Comparisons with the DIT and CoMD calculations indicated an overall fair description. Moreover, our future steps include detailed study of other reaction channels of the ^{64}Ni on ^{64}Ni system, as well as investigation of the excitation energy distributions in parallel to the momentum distributions in order to deepen our understanding of the reaction mechanisms at this energy regime.

References

[1] J. J. Cowan, C. Sneden, J. E. Lawler, A. Aprahamian, M. Wiescher, K. Langanke, G. Martínez-Pinedo, and F. Thielemann. "Origin of the heaviest elements: The rapid neutron-capture process". In: *Rev. Mod. Phys.* 93 (2021), p. 015002. DOI: 10.1103/RevModPhys.93.015002.

[2] G. G. Adamian, N. V. Antonenko, A. Diaz-Torres, and S. Heinz. "How to extend the chart of nuclides?" In: *Eur. Phys. J. A* 56 (2020), p. 47. DOI: 10.1140/epja/s10050-020-00046-7.

[3] S. Koulouris et al. "Multinucleon transfer channels from ^{70}Zn (15 MeV/nucleon) + ^{64}Ni collisions". In: *Phys. Rev. C* 108 (2023), p. 044612. DOI: 10.1103/PhysRevC.108.044612.

[4] O. Fasoula, G. A. Souliotis, S. Koulouris, K. Palli, M. Veselsky, S. J. Yennello, and A. Bonasera. "Momentum distribution studies of projectile fragments from peripheral collisions below the Fermi energy". In: *HNPS Adv. Nucl. Phys.* 29 (2023), pp. 38–44. DOI: 10.12681/hnpsanp.5089.

[5] K. Palli, G. A. Souliotis, T. Depastas, I. Dimitropoulos, O. Fasoula, S. Koulouris, M. Veselsky, S. J. Yennello, and A. Bonasera. "Microscopic dynamical description of multinucleon transfer in ^{40}Ar induced peripheral collisions at 15 MeV/nucleon". In: *EPJ Web Conf.* 252 (2021), p. 07002. DOI: 10.1051/epjconf/202125207002.

[6] L. Tassan-Got and C. Stephan. "Deep inelastic transfers: a way to dissipate energy and angular momentum for reactions in the Fermi energy domain". In: *Nucl. Phys. A* 524 (1991), pp. 121–140. DOI: 10.1016/0375-9474(91)90019-3.

[7] M. Papa, T. Maruyama, and A. Bonasera. "Constrained molecular dynamics approach to fermionic systems". In: *Phys. Rev. C* 64 (2001), p. 024612. DOI: 10.1103/PhysRevC.64.024612.

[8] R. J. Charity et al. "Systematics of complex fragment emission in niobium-induced reactions". In: *Nucl. Phys. A* 483 (1988), pp. 371–405. DOI: 10.1016/0375-9474(88)90542-8.

[9] G. A. Souliotis, D. V. Shetty, A. Keksis, E. Bell, M. Jandel, M. Veselsky, and S. J. Yennello. "Heavy-residue isoscaling as a probe of the symmetry energy of hot fragments". In: *Phys. Rev. C* 73 (2006), p. 024606. DOI: 10.1103/PhysRevC.73.024606.

[10] G. A. Souliotis, B. Stein, M. Veselsky, S. Galanopoulos, A. L. Keksis, Z. Kohley, D. V. Shetty, S. N. Soisson, S. Wuenschel, and S. J. Yennello. "Neutron-rich rare isotope production in the Fermi energy domain and application to the Texas A&M radioactive beam upgrade". In: *Nucl. Instrum. Meth. Phys. Res. B* 266 (2008), pp. 4692–4696. DOI: 10.1016/j.nimb.2008.05.118.

[11] E. Kontogianni, G. A. Souliotis, C. Giannitsa, K. Gkatzogias, N. Korakis, S. Koulouris, E. Travlou, M. Veselsky, S. J. Yennello, and A. Bonasera. "Projectile fragments from peripheral collisions of 25 MeV/nucleon ^{64}Ni on ^{64}Ni". In: *EPJ Web of Conf.* 304 (2024), p. 01016. DOI: 10.1051/epjconf/202430401016.